energies

MDPI

Article

Influence of the Calcination Temperature of Synthetic Gypsum on the Particle Size Distribution and Setting Time of Modified Building Materials

Artur Koper [1], Karol Prałat [1,*], Justyna Ciemnicka [1] and Katarzyna Buczkowska [2,3]

1 Institute of Building, Faculty of Civil Engineering, Mechanics and Petrochemistry, Warsaw University of Technology, Łukasiewicza Street 17, 09-400 Płock, Poland; Artur.Koper@pw.edu.pl (A.K.); Justyna.Ciemnicka@pw.edu.pl (J.C.)

2 Department of Material Science, Faculty of Mechanical Engineering, Technical University od Liberec, Studentska Street 2, 461-17 Liberec, Czech Republic; Katarzyna.Ewa.Buczkowska@tul.cz

3 Department of Materials Technology and Production Systems, Faculty of Mechanical Engineering, Lodz University of Technology, Stefanowskiego Street 1/15, 90-537 Łódź, Poland

* Correspondence: Karol.Pralat@pw.edu.pl

Received: 12 October 2020; Accepted: 28 October 2020; Published: 3 November 2020

Abstract: The paper assesses the influence of the calcination temperature of synthetic gypsum binder on the binding properties of innovative gypsum pastes, as well as on masonry and plastering mortars. The calcination process of gypsum binder was carried out at four different temperatures ranging from 170 to 190 °C. The specimens for testing were prepared on the basis of the obtained raw material with a constant water to gypsum ratio of w/g = 0.75. It was noted that the calcination temperature influenced the setting time of the gypsum. Based on synthetic gypsum, mixtures of masonry and plastering mortars modified with tartaric acid and Plast Retard were designed. During the experiment, the particle diameter distribution of aqueous suspensions of building and synthetic gypsum particles (before and after calcination) was determined using the Fraunhofer laser method. The dimensions of the obtained artificial gypsum grains did not differ from the diameters of the gypsum grains in the reference sample. On the basis of the conducted research, it was found that the waste synthetic gypsum obtained in the flue gas desulphurization process met the standard conditions related to its setting time. Therefore, it may be a very good construction substitute for natural gypsum, and consequently, it may contribute to environmental protection and the saving and respecting of energy.

Keywords: synthetic gypsum; calcination process; setting time; Fraunhofer method; particle size distribution

1. Introduction

Gypsum is a commonly used building material. It is characterized by its lower natural radioactivity in the group of mineral construction binding materials, as well as by its quick growth of strength [1]. The development of the construction industry and the growing demand for more and more ecological and perfect building materials has led to the searching for new solutions to improve these materials. Due to growing ecological awareness, new methods of waste management in various branches of industry are being developed.

Gypsum can be modified with the use of various chemical additives. Such additives can be, among others, accelerants, retarders, glass fibers, cellulose fibers, vermiculite, aerogels, microspheres polymers, and copolymers [2–6]. All such modifications affect the properties of gypsum composite and its application.

One of the most important environmental problems is air pollution with sulfur oxides that result from the combustion of fossil fuels. For this reason, measures that aim to reduce the emission of harmful substances generated as a by-product of combustion are a very big challenge. One of the main ways to neutralize the impact of pollutants on the environment is by using the flue gas desulphurization process, the by-product of which is synthetic gypsum. In order to meet social expectations, the pro-ecological construction industry recognizes the possibility of replacing natural gypsum with synthetic gypsum.

Currently, a very broad field of science within innovative and pro-environmental material solutions concerns the properties of synthetic gypsum obtained in the flue gas desulphurization process [7–11]. However, before its commercial use, it is necessary to perform a series of tests and studies. In this area, science and industry strive to obtain construction products with the most suitable expected parameters, e.g., thermal, strength, mechanical or other. A very important property of building materials is their setting time. It is the time from the moment the binder is moistened and mixed, in which the grout maintains plastic properties, until the final material is sufficiently hardened. The setting time depends on the type of binder, and also the amount of mixing water and its temperature [12–15].

The basic process used in the construction industry for the production of synthetic gypsum is the calcination process. In the entire production process, this stage is the most energy consuming and involves the heating of the substance below its melting point in order to cause a partial chemical decomposition of the compound by removing water from its crystal lattice. In the case of gypsum, it causes the processing of dihydrate calcium sulphate into a semi-aqueous or anhydrous form. The calcination process itself takes place with the use of various methods and calcination boilers [16–22]. The obtained dihydrate calcium sulphate may undergo internal changes under the influence of temperature (Figure 1).

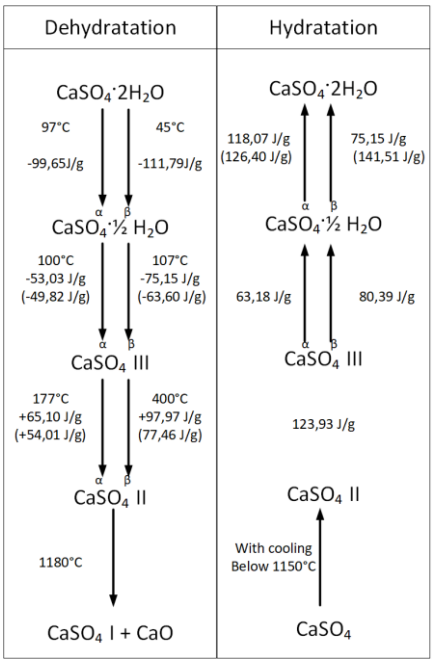

Figure 1. Possible transformations of the dehydration and hydration of synthetic gypsum in the calcination process [23].

The dehydration process takes place successively over a period of time and depends on many factors, mainly including the method of calcination, the granulation of the pure raw material, and the presence of minerals and other chemical compounds. The type of predominant dehydrate phase and the properties of the binder depend on the applied temperature changes. Usually, there are various transition phases in the final product, which correspond to the calcination temperature range. This

effect is influenced by wide equilibrium temperature ranges in the process of the transformation of dihydrate gypsum into semi-aqueous gypsum and anhydrite.

In the process of the dehydration of β phases, the instability of the $CaSO_4$-H_2O system occurs at a temperature of 45 °C. The first intense dehydration of the dihydrate into hemihydrate occurs in the temperature range of 107–170 °C (Figure 1). The transition of the hemihydrate into the unstable phase of anhydrite III in the β phases takes place in the temperature range of 170–180 °C, followed by the occurrence of intense changes at a temperature close to 200 °C. The conversion of anhydrite III into sparingly soluble anhydrite II takes place at a temperature of about 400 °C in the case of theβ hemihydrate. At temperatures above 600 °C, the decomposition of calcium sulphate begins according to reaction (1).

$$CaSO_4 \quad CaO + SO_2 + 0.5O_2 \tag{1}$$

The product obtained from this stage, which contains 2–3% of unbound CaO, is a raw material for the production of estrich gypsum. With a rapid increase in temperature and large grains, non-dehydrated material may remain in the raw material, which can be seen in the analysis of the mineral composition of building gypsum (β hemihydrate). The above factors affect the heterogeneity of products obtained in the calcination process and, consequently, the differentiation of the properties of gypsum binders.

It has been documented that the dehydration process, from the dihydrate phase to the anhydrite II phase, is accompanied by significant changes in the crystal structure Equation (2), and large changes in density from 2.31 to 2.98 g/cm^3, respectively [23].

$CaSO_4 \cdot 2H_2O$	$CaSO_4 \cdot 0.5H_2O$	$CaSO_4$ III	$CaSO_4$ II
monoclinic	monoclinic	pseudo-hexagonal	orthorhombic

(2)

Due to its more difficult workability, synthetic gypsum requires the use of various specially selected admixtures to modify its properties. Innovative recipes for masonry and plastering mortars are created experimentally by selecting the components in an optimized way.

The aim of the study was to evaluate the effect of the calcination temperature of synthetic gypsum binder on the binding properties of innovative gypsum pastes, as well as on the properties of masonry and plastering mortars. A63 tartaric acid and a compound delaying the binding—Plast Retard—were used when creating recipes for mortars based on synthetic gypsum that was obtained from flue gas desulphurization. An additional goal was to analyze the grain size of the synthetic gypsum before and after the calcination process and to determine the effect of this process on the grain diameters of the obtained building materials. The authors' intention was also to compare the particle size measurements of the gypsums obtained from flue-gas desulphurization with the results obtained for building gypsum (reference material). The authors of the study assume that construction materials based on synthetic gypsum do not have different properties than materials based on natural gypsum. The use of synthetic gypsum in building materials would have a significant economic impact. Currently, a lot of synthetic gypsum is deposited in flue gas desulphurization plants as waste. Its recycling would bring benefits for environmental engineering, as well as contribute to the reduction of the energy-intensive process of obtaining natural gypsum. Such activities will surely be beneficial for global energy saving and ecology.

2. Materials and Methods

2.1. Materials Used in the Research

2.1.1. Building Gypsum

The material applied during the research was building gypsum (Dolina Nidy, Pinczow). This gypsum is used in construction, renovation and completion works inside buildings. It is used for the production of mortars and prefabricated elements [24].

Gypsum materials, apart from their ability to maintain hygrothermal balance in buildings, are fire resistant, environmentally friendly and almost odorless. Additionally, they can be seen as very good acoustic and thermal materials. Therefore, gypsum plasters applied in rooms are very aesthetic and provide comfort of living. Natural gypsum can be excavated from mines, whereas its synthetic version can be obtained by the chemical synthesis during the flue-gas desulfurization process. Both types have different physical properties and can be used interchangeably in the construction industry.

Natural gypsum is a mineral binding material, which is extracted during the process of partial dehydration of natural gypsum stone (dihydrate calcium sulphate) from an opencast gypsum mine. It is characterized by the quick growth of mechanical strength and short time of binding.

The natural gypsum, which is commercially available and meets the standard requirements, was used as the reference material. The content of calcium sulfate ($CaSO_4$) in the gypsum powder was almost 91%, and the additional ingredients included: $CaCO_3$—2.79%, SiO_2—1.62%, montmorillonite—3.07%, clays—0.79%, and chlorite—0.16%. Table 1 summarizes the basic physical properties of the building materials that were used in the tests. These parameters were obtained from safety data sheets made available by the producer [24].

Table 1. Basic physical properties of the building gypsum used in the tests [24].

Building Material	Density d (kg·m^{-3})	Bulk Density d_B (kg·m^{-3})	pH	Color	Appearance	Setting Time (min)
Building gypsum	2300	900	7/8	grey	grey-yellow powder	3

2.1.2. Synthetic Gypsum

The synthetic gypsum (Nova-gypsum) that was used in the research was obtained using the wet lime method. Currently, there are many known industrial methods for the production of synthetic dihydrate gypsum [25–28]. The most used flue gas desulphurization method in the world is the wet limestone method that uses limestone ($CaCO_3$) or quicklime (CaO). It involves the absorption of SO_2 in an aqueous suspension of limestone flour. The cooled raw flue gas is directly injected into water, and then redirected to the absorbent where SO_2 is washed out and sulfites are formed. In the next stage, oxidation of sulfite ions takes place and the precipitation of synthetic gypsum dihydrate $CaSO_4$ $2H_2O$ occurs. The chemical reaction of the flue gas desulphurization process and the production of synthetic dihydrate gypsum takes place in the following stages:

$$CaCO_3 + 2H^+ \quad Ca^{2+} + H_2O + CO_2 \tag{3}$$

$$CaO + H_2O \quad Ca^{2+} + 2OH^- \tag{4}$$

$$Ca^{2+} + 2HSO_3^- + O_2 + 4H_2O \quad 2CaSO_4\ 2H_2O + 2H^+ \tag{5}$$

The created gypsum paste is thickened and collected as a powder with a moisture content of about 10%. Harmful impurities are removed from the product by rinsing. Synthetic building gypsum has a similar chemical composition and similar properties to natural gypsum, but mainly in its hardened state. However, its compressive strength is greater than that of natural gypsum (by about 35–40%). It has low grain cohesion (different graining), and is therefore also less workable. It can be recognized by its slightly creamy color. Some of its properties cause many technological problems for industrial recipients, and thus this gypsum, depending on the types of manufactured products, requires the use of various specially selected modifying admixtures. Currently, this gypsum, as is the case with natural gypsum, is used as a full-value material for the production of various products.

2.1.3. Tartaric Acid

Tartaric acid is a product belonging to the group of dicarboxylic hydroxy acids that contain two hydroxyl groups (−OH). It fulfils a number of functions in various areas of life, e.g., in the pharmaceutical and food industries [29–34]. In the construction industry, it is used as a retarder in the preparation of gypsum mortars. Tartaric acid is in the form of colorless crystals or white powder, and is almost odorless, strongly sour in taste, stable in air, and hygroscopic at a relative humidity higher than 75%. According to the manufacturer's data, it has the properties listed in Table 2 [35].

Table 2. Properties of the tartaric acid used in the research [35].

Solubility at 25 °C in 100 cm^3			Solid Density	Apparent Density	Melting Temperature
of water (g)	of ethanol (g)	of ether (g)	ρ_s (kg/m^3)	ρ_a (kg/m^3)	T_m (°C)
147	33	0.4	1760	800/1100	168/170

The use of tartaric acid increases the plasticity and strength of concrete [36–38]. The used A63 tartaric acid (Evimex Ltd., Tomaszów Mazowiecki, Poland) contained a maximum of 1% of particles with a size greater than 0.063 mm in its composition.

2.1.4. Plast Retard

This material belongs to the group of admixtures that delay the binding time of gypsum by slowing down the growth of hydrate crystals. It can be used with natural gypsum, flue-gas gypsum, and phosphogypsum of a low or high quality and with different water to gypsum ratios (w/g). Its use can extend the mixing time of the mixture by up to several hours and reduce the risk of thermal stresses during binding. Plast Retard (Evimex Ltd.) is in the form of a fine, highly water-soluble, hygroscopic, and light-colored powder. Chemically, it is calcium salts of reduced polyamides. Due to its properties [39], mainly its thermal stability up to 300 °C, it can be used in a wide temperature range. It also works very well with other additives, e.g., tartaric acid. The basic properties of this admixture are presented in Table 3.

Table 3. Properties of the Plast Retard used in the research [39].

Color	Physical Form	pH in a 10% Solutions	Apparent Density	Active Substances	Water Content
(–)	(–)	(–)	ρ_a (kg/m^3)	(%)	(%)
White	Solid, powder	8	300	>95	<5

Plast Retard acts as a retarder in the gypsum-water mixture, slowing down the growth of the hydrate crystals. Its activity is characterized by the correlation between setting time and dosage, and it gives excellent performance even at low dosage rates. Generally, Plast Retard is used alone in gypsum formulations, but it is also compatible with citric acid and tartaric acid when being used to obtain a delayed hardening and suitable consistency.

2.1.5. Other Ingredients

In addition to the basic ingredients of innovative masonry and plastering mortars (synthetic gypsum, Plast Retard, tartaric acid), admixtures also include: river sand with a grain diameter of 0–2 mm, methylcellulose, lime flour, perlite, hydrated lime, and water.

2.2. Measurements of Particle Diameters

The main assumptions of the Fraunhofer theory are shown in article [40]. In the case when a laser beam hits a single particle, the light diffracts. This phenomenon can be described using the Fraunhofer theory and is possible if the particle fulfills the condition of x ≫ 1 (x = πd/λ, d—particle diameter).

Taking into account the assumptions of Babinet and Fraunhofer, Airy described this phenomenon using Relationship (6):

$$I(\theta, x) = I_0 \frac{\pi^2 d^4}{16F^2\lambda^2}\left[\frac{2J_1(xsin\theta)}{xsin\theta}\right]^2 \quad (6)$$

where: I_0—is the intensity of light, θ—is the diffraction angle, F—is the focal length of the lens. When assuming that the sine of the angle θ is very small ($sin\theta \approx \theta$), the following Relationship (7) is obtained:

$$I(\theta, x) = I_0 \frac{\pi^2 d^4}{16F^2\lambda^2}\left[\frac{2J_1(x\theta)}{x\theta}\right]^2 \quad (7)$$

If the tested sample has a very small concentration of particles, then such a sample meets the condition for a single scattering. Therefore, the above equation can be integrated within the particle size range, which results in the obtaining of the diffraction intensity distribution that is described by the Fredholm integral Equation (8) [40,41]:

$$I(\theta) = I_0 \int_0^\infty \frac{\pi^2 d^4}{16F^2\lambda^2}\left[\frac{2J_1(x\theta)}{x\theta}\right]^2 n(x)dx = I_0 \int_0^\infty \frac{J_1^2(x\theta)x^2 n(x)}{F^2k^2\theta^2}dx \quad (8)$$

Due to the mathematical foundations of Fraunhofer, the advanced optical systems, and the development of laser techniques, it was possible to conduct measurements based on the diffractometric method.

The system that is used to analyze optical images consists of the following elements: a laser, an advanced optical system, a measuring cell, lenses, and an image detector. The image of the light diffraction grating, which was formed at the edge of the grains suspended in the water, was recorded and saved by a computer. The diffraction method is commonly used in industry for the purpose of measuring grain diameters, and also as an element of testing the quality of manufactured products in the pharmaceutical, food and construction industries [42–45].

A detailed description of image processing in a granulometer, as well as a description of the resulting diffraction image, are described in publications [46,47]. It should be mentioned that the identification of the grain diameter involves the measuring of the distance between the strip and the optical axis, as well as the measuring of the brightness of the diffraction strip. From the obtained image, it can be concluded that the greater the distance between the stripe and the optical axis, the smaller the size of the examined grains. It can also be stated that a higher brightness intensity of the stripes correlates with a larger amount of grains with particular dimensions in the entire sample.

An Analysette 22 MicroTec Plus particle size analyzer produced by FRITSCH GmbH (Katowice, Poland) Milling and Sizing, which consists of green and infrared lasers, was applied when analyzing the size of the particles. It uses an inverse Fourier system according to ISO 13320, and has a modular structure that includes a measuring unit and units for the preparation of samples for wet or dry measurements. The particle size analyzer that was applied in the research took measurements of the granulation of the suspension of particles in water. It consisted of two units—a larger one, which was the main measuring part, and a smaller one, which was the dispersing unit. Grains with a diameter within the range between 0.08 and 2100 µm can be measured in the device. Measurements of particle size distribution using the particle size analyzer, a computer, and the diffractometric method are very precise, and the applied apparatus does not require any calibration on the basis of the basic physical properties.

2.3. Setting Time Measurement

The setting time of the gypsum materials was tested using the Vicat method in accordance with the guidelines contained in PN-EN 13279-2 [48]. It is a method intended for gypsum plasters in the form of dry mixtures that also contain additives, among others, retard ingredients. It involves the penetration of an immersion cone (with specified dimensions and mass) in the mortar (Figure 2). The immersion depth of the cone is a measure of the progress of the setting process. A detailed description of the research methodology can be found in [49].

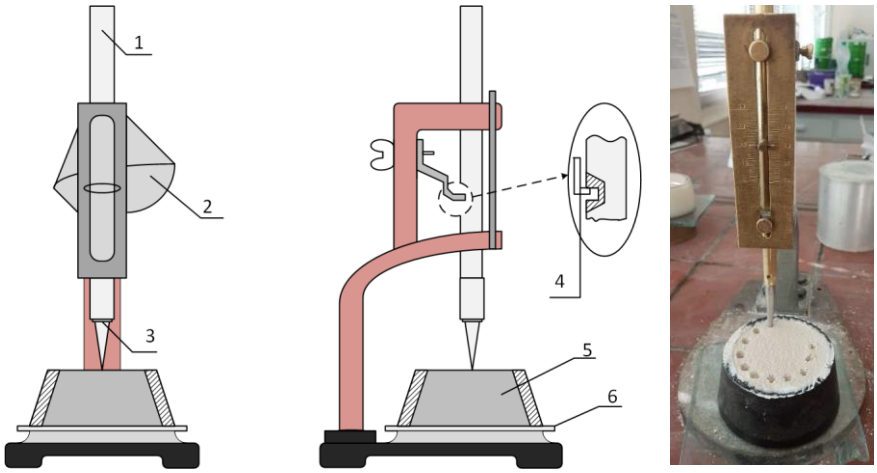

Figure 2. The Vicat apparatus used in the tests: (**a**) diagram and (**b**) photo: 1—guide, 2—release mechanism, 3—immersion cone, 4—resilient plate, 5—Vicat ring, 6—glass plate.

2.4. Gypsum Pastes Used in the Research

In the study of gypsum pastes, a constant water to gypsum ratio of w/g = 0.75 was used, which was determined experimentally using the slump test. The test was carried out in accordance with the PN-EN 13279-2 standard, which is used for pastes, mortars and gypsum plasters with a liquid consistency. The tests involve the measuring of the sample's slump diameter. For the purposes of investigating the effect of the gypsum calcination temperature on the setting time of the pastes, four samples were prepared. They contained synthetic gypsum that was obtained at different calcination temperatures: 170, 180, 185 and 190 °C for 7 h. Additionally, for comparison purposes, a reference sample containing building gypsum instead of synthetic gypsum was prepared. In all cases, a slump diameter of 175 mm was obtained. The amounts of ingredients and the results of the slump diameters obtained using the slump test are presented in Table 4.

Table 4. List of the types of tested gypsum pastes.

Gypsum Paste Ingredients	Amount of Components (g)
	BG, SG170, SG180, SG185, SG190 *
Water	230
Gypsum	300
The obtained diameter of the slump for the determination of consistency (mm)	175

* signs: BG–building gypsum; SG—synthetic gypsum; 170, 180, 185, 190—calcination temperature.

2.5. New Masonry and Plastering Mortars on the Basis of Retardan and A63 Tartaric Acid

Based on the granulation tests and the setting time of the gypsum pastes, recipes for masonry and plastering mortars, which are based on synthetic gypsum and meet the standard requirements, were designed. As was the case with the gypsum pastes, in order to determine the effect of the gypsum binder's calcination temperature on the setting time of the modified masonry and plastering mortars, four types of mortars based on synthetic gypsum, and one reference mortar based on the building gypsum, were prepared. Additionally, the mortar recipes were diversified by using two types of gypsum setting retarders (Plast Retard and A63 tartaric acid). The recipes of the prepared mortars are presented in Table 5 for masonry mortars, and in Table 6 for plastering mortars.

Table 5. The obtained recipes of the masonry mortars [50].

Mortar Ingredients		Designations of Mansonry Mortars				
		MBG	**MSG170**	**MSG180**	**MSG185**	**MSG190**
With the addition of Plast Retard						
Gypsum	(g)	700.00	700.00	700.00	700.00	700.00
Vistula sand 0–2 mm		245.50	245.98	245.95	246.04	246.13
Methylcellulose		3.00	3.00	3.00	3.00	3.00
Hydrated lime		50.00	50.00	50.00	50.00	50.00
Plast Retard		1.50	1.02	1.05	0.96	0.87
Water		550.00	620.00	620.00	620.00	620.00
With the addition of tartaric acid A63						
Gypsum	(g)	700.00	700.00	700.00	700.00	700.00
Vistula sand 0–2 mm		246.64	246.58	246.61	246.64	246.58
Methylcellulose		3.00	3.00	3.00	3.00	3.00
Hydrated lime		50.00	50.00	50.00	50.00	50.00
Tartaric acid A63		0.36	0.42	0.39	0.36	0.42
Water		550.00	620.00	620.00	620.00	620.00

signs: MBG—mortar based on building gypsum, MSG—mortar based on synthetic gypsum.

Table 6. The obtained recipes of the plastering mortars [50].

Mortar Ingredients		Designations of Plastering mortars				
		PMBG	**PMSG170**	**PMSG180**	**PMSG185**	**PMSG190**
With the addition of Plast Retard						
Gypsum	(g)	700.00	700.00	700.00	700.00	700.00
Limestone flour		221.15	221.04	220.86	221.04	221.04
Methylcellulose		4.00	4.00	4.00	4.00	4.00
Perlite		34.00	34.00	34.00	34.00	34.00
Methylcellulose		40.00	40.00	40.00	40.00	40.00
Plast Retard		0.85	0.96	1.14	0.96	0.96
Water		800.00	860.00	860.00	860.00	860.00

Table 6. *Cont.*

Mortar Ingredients		Designations of Plastering mortars				
		PMBG	**PMSG170**	**PMSG180**	**PMSG185**	**PMSG190**
With the addition of tartaric acid A63						
Gypsum	(g)	700.00	700.00	700.00	700.00	700.00
Limestone flour		221.58	221.58	221.61	221.64	221.65
Methylcellulose		4.00	4.00	4.00	4.00	4.00
Perlite		34.00	34.00	34.00	34.00	34.00
Methylcellulose		40.00	40.00	40.00	40.00	40.00
Tartaric acid A63		0.42	0.42	0.39	0.36	0.35
Water		800.00	860.00	860.00	860.00	860.00

signs: PMBG—plastering mortar based on building gypsum, PMSG—plastering mortar based on synthetic gypsum.

3. Research Results and Analysis

3.1. Results of Particle Size Distribution

All the studied samples of building materials were characterized by good wettability. During the experimental tests, in all the cases, the power of the pumps was used at 60% capacity, and the power of light and ultrasound at 100%. In the first 10 s of the measurements, the air bubbles were removed and the time it took for each sample to be added to the dispersing part of the device was no longer than 30 s. Each gypsum material was measured three times.

On the basis of the collected measurement data, it was found that very high repeatability was obtained in subsequent measurements for the building gypsum (Figure 3a) and the synthetic gypsum before calcination (Figure 3b). The distribution of the particle diameter of the synthetic gypsum after the calcination process was not repeatable during the measurements. The first sample contained particles with a diameter of 100–1000 µm, which were not noticeable in the second and third measurements. This indicates the formation of agglomerates, and also the agglomeration of the particles into larger clusters that occur during the calcination process. As a result of the influence of water, there was a division of these particles in the measuring system, which was noticeable in the second and third measurements (Figure 3c).

The synthetic gypsum before the calcination process was characterized by a larger particle size ranging from 10 to 100 µm (Figure 3b) when compared to the building gypsum, which had particles with diameters from 0.1 to 40 µm (Figure 3a). The calcination process (Figure 3c) caused the diameters of the synthetic gypsum to be reduced to values similar to the building gypsum. The influence of the calcination process on the grain size was noticed by the author of paper [50], who presented his views in a photo (Figure 4).

(**a**)

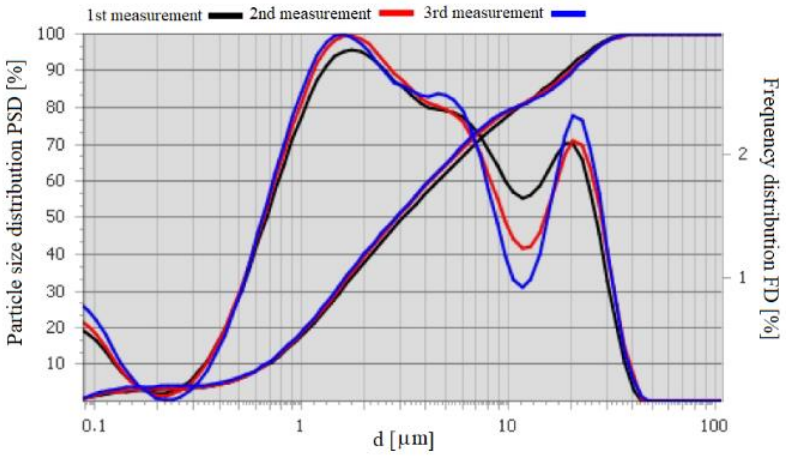

(**b**)

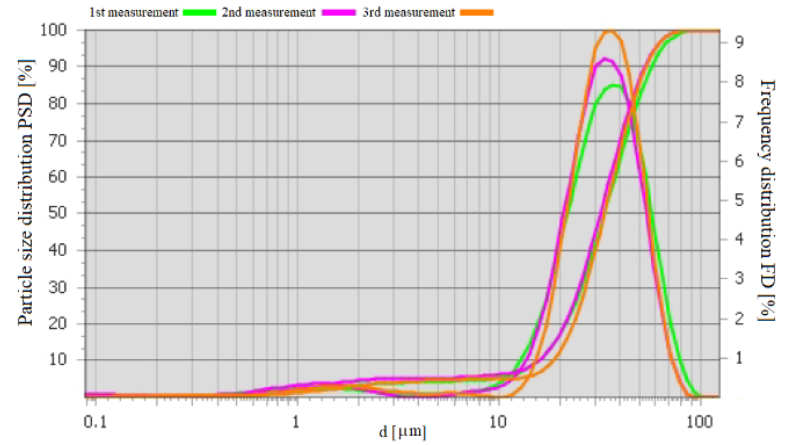

(**c**)

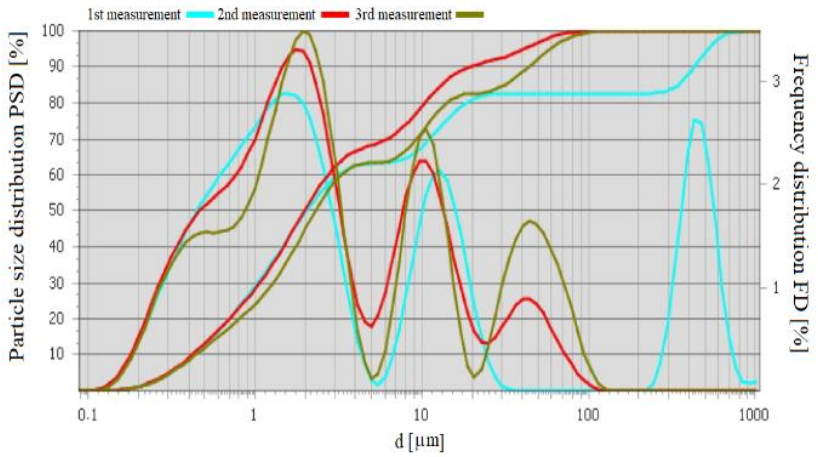

Figure 3. Graph of dependency $PSD = f(d)$ for the studied building materials: (**a**) building gypsum, (**b**) artificial gypsum before the calcination process, (**c**) artificial gypsum after the calcination process.

Figure 4. The appearance of gypsum: (**a**) before the calcination process, (**b**) after the calcination process [50].

Schaefer et al. [51] showed that phosphogypsum subjected to the calcination process in the temperature range of 350–650 °C was characterized by particle diameters from 10 to 40 µm. The authors noticed that the different values of the calcination process temperatures did not significantly affect the obtained diameters of the phosphogypsum. Salih and Hussein [52] obtained gypsum after the calcination and grinding processes that contained particles with a diameter from 0.5 to 45 µm, and Cakal et al. [53] obtained average particle diameters of 37–41 µm. The authors of [54] note that gypsum after the calcination process, in order to have appropriate properties for the construction industry, should have particles smaller than 10 µm in an amount of up to 70%. Klin [1] declares a very good plaster quality if there is 44% of grains with diameters ranging from 0 to 40 µm.

The results of statistical parameters of all the gypsum materials are presented in the Figures 5–7: diameters of characteristic grains d_{10}, d_{50}, d_{90}, mode and span. The span is described by Equation (9):

$$Span = \frac{d_{90} - d_{10}}{d_{50}} \quad (9)$$

In the case of the obtained statistical data for the commercial building gypsum (Figure 5a–c), it can be stated that the diameters of the particles that have the highest probability of occurring in this building material are in the range of 1.69–1.76 µm.

The synthetic gypsum before the calcination process had the most particles in the range of 33.69–38.04 µm (Figure 6a–c), while after the calcination process it had the most particles within the range of 1.56–1.99 µm (Figure 7a–c). The experimental results showed that the calcination process caused the reduction of the average grain diameters of the synthetic gypsum to be comparable to the values obtained for the reference sample (building gypsum). Moreover, the D_{50} values for the building gypsum and synthetic gypsum after the calcination process were 2.9 and 2.1 µm, respectively, which proves the similar particle size properties of both products.

(**a**)

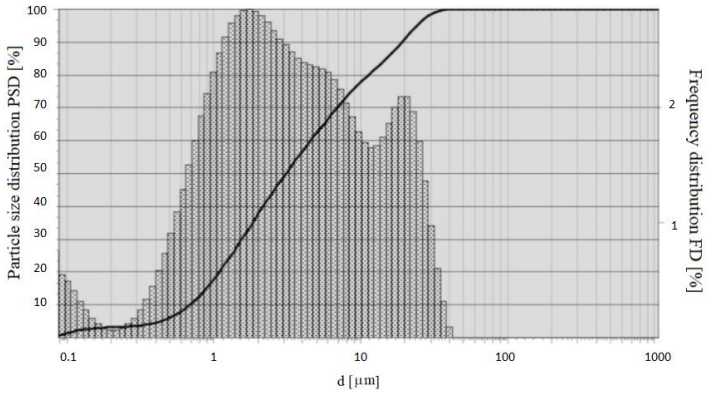

Statistical parameters	
d_{10} [µm]	0.7
d_{50} [µm]	2.9
d_{90} [µm]	19.8
modal [µm]	1.76
span [-]	5.92

(**b**)

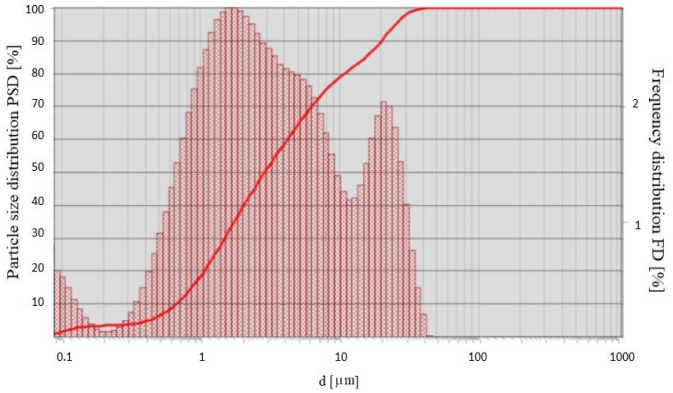

Statistical parameters	
d_{10} [µm]	0.7
d_{50} [µm]	2.9
d_{90} [µm]	20.0
modal [µm]	1.71
span [-]	6.71

(**c**)

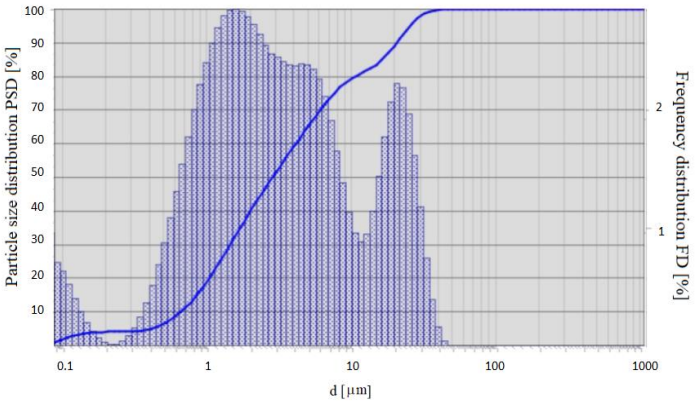

Statistical parameters	
d_{10} [µm]	0.7
d_{50} [µm]	2.8
d_{90} [µm]	20.5
modal [µm]	1.69
span [-]	7.00

Figure 5. Sizes of characteristic particles determined with the use of the laser diffraction method in the samples of building gypsum: (**a**) 1st measurement, (**b**) 2nd measurement, (**c**) 3rd measurement.

(**a**)

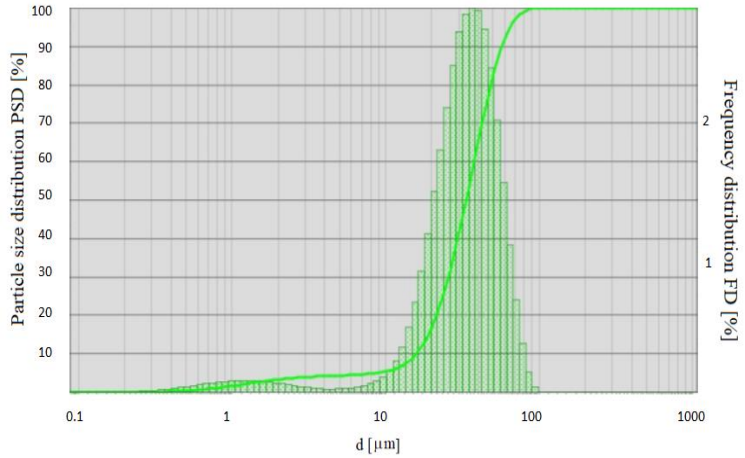

Statistical parameters	
d_{10} [µm]	15.8
d_{50} [µm]	33.5
d_{90} [µm]	57.1
modal [µm]	38.04
span [-]	1.23

(**b**)

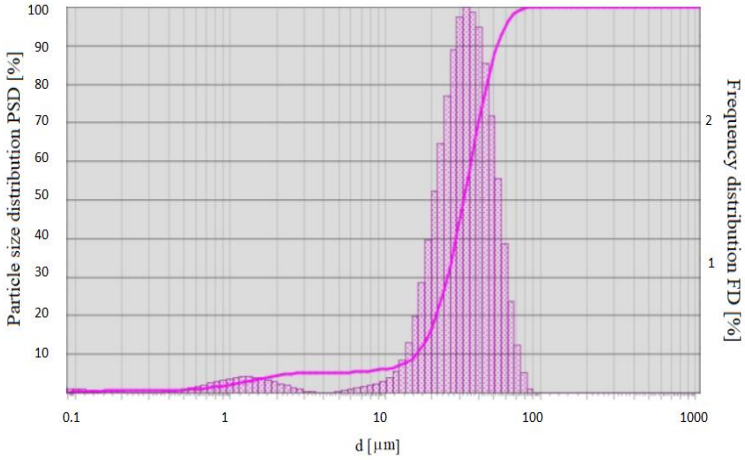

Statistical parameters	
d_{10} [µm]	15.8
d_{50} [µm]	32.0
d_{90} [µm]	52.9
modal [µm]	33.69
span [-]	1.15

(**c**)

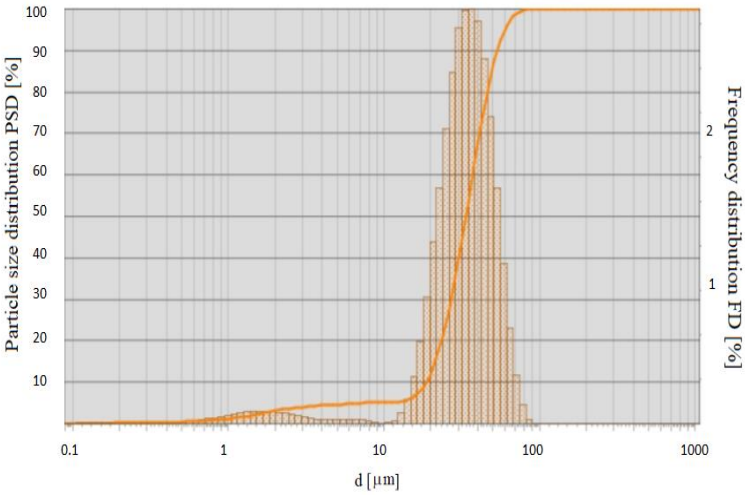

Statistical parameters	
d_{10} [µm]	18.6
d_{50} [µm]	33.5
d_{90} [µm]	53.5
modal [µm]	34.73
span [-]	1.03

Figure 6. Sizes of characteristic particles determined with the use of the laser diffraction method in the samples of synthetic gypsum before the calcination process: (**a**) 1st measurement, (**b**) 2nd measurement, (**c**) 3rd measurement.

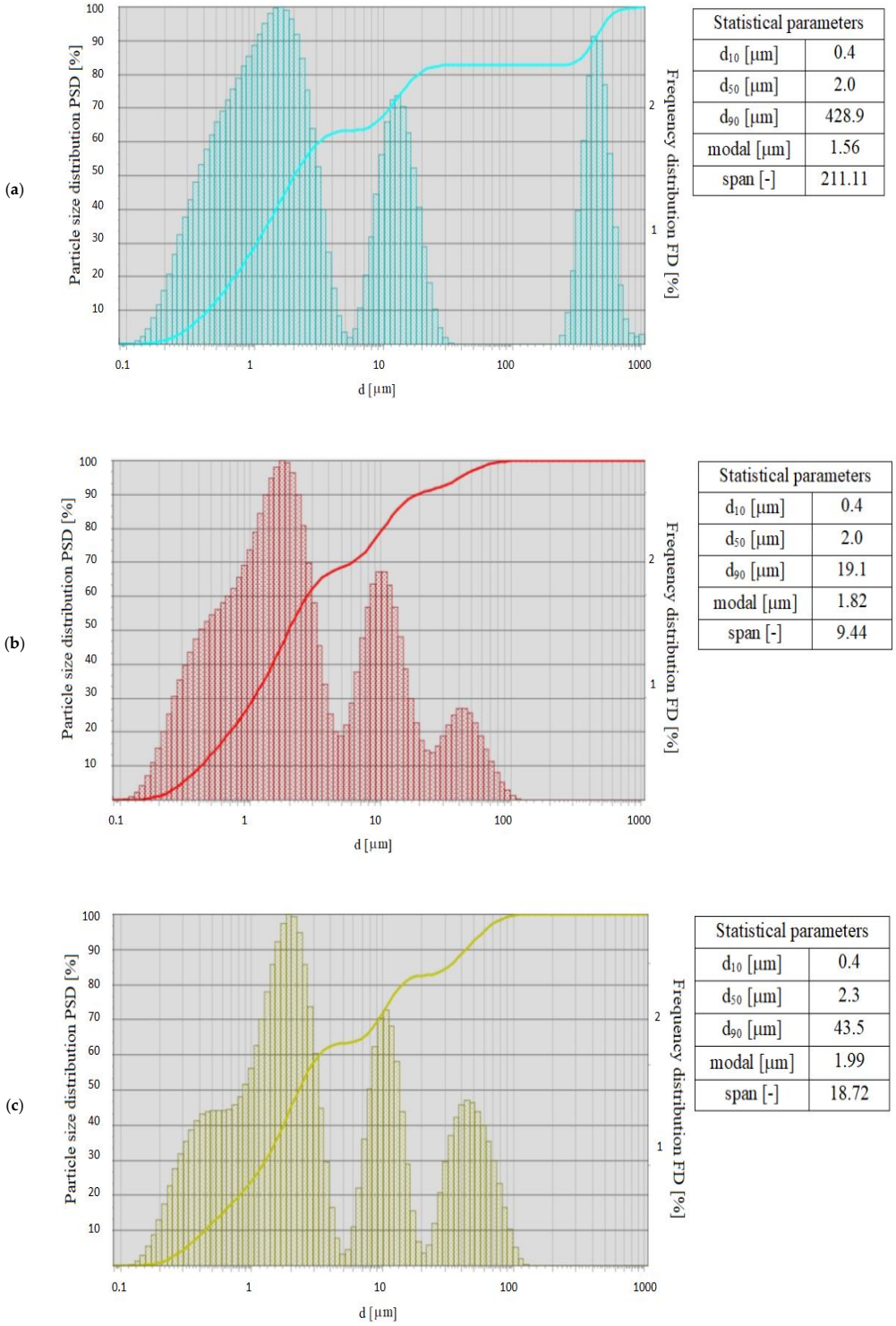

Figure 7. Sizes of characteristic particles determined with the use of the laser diffraction method in Table 1: (**a**) 1st measurement, (**b**) 2nd measurement, (**c**) 3rd measurement.

The authors of papers [1,51,52] emphasize the fact that for the proper use of new building materials, particle diameters below 10 µm should constitute a significant part of all the particles in the used gypsum materials. Additionally, Borgwardt [54] points out that the diameters of gypsum particles with dimensions of 10 µm extend the calcination time by five times when compared to particles with

dimensions of 1 µm, and also that particles with dimensions of 90 µm extend the calcination time by up to ten times.

In the present study, in the synthetic gypsum that was obtained after the calcination process, 75–80% of the grains have a diameter smaller than that required. The obtained product, derived from flue gas desulphurization and then subjected to thermal treatment, can therefore be a substitute for commercial building gypsum. Figure 8a–c show the results of all the studied building materials, and present the average particle size distribution as a function of grain diameter.

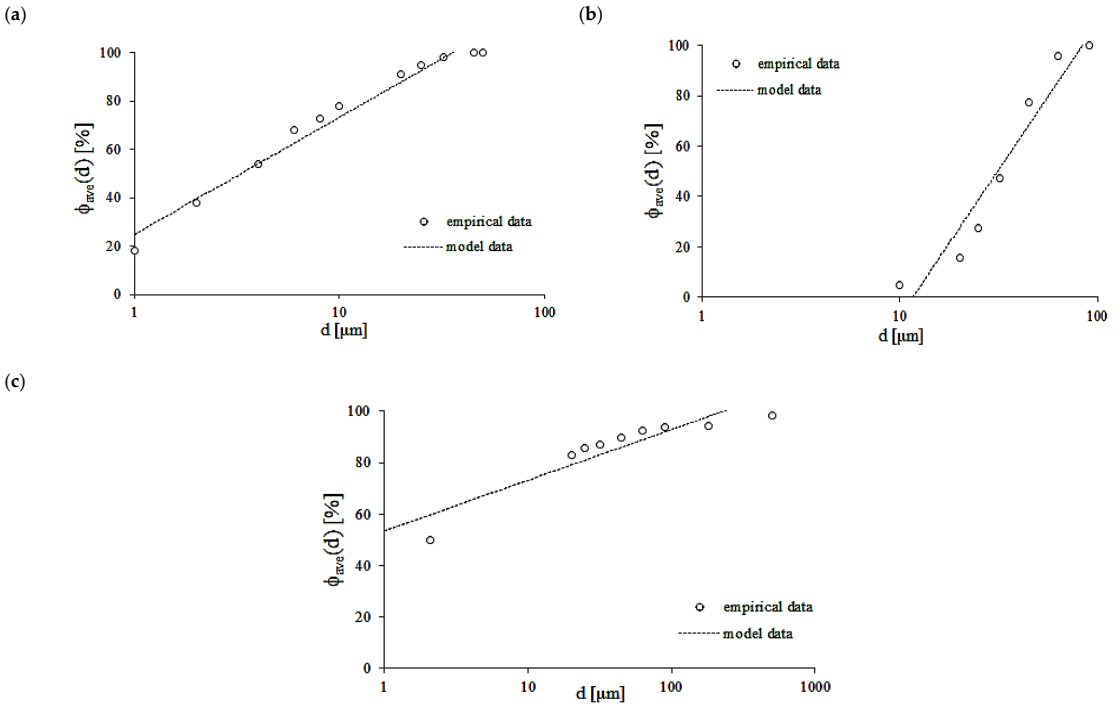

Figure 8. Results of the average particle distribution of the gypsums tested using laser diffraction: (**a**) building gypsum, (**b**) synthetic gypsum before calcination, (**c**) synthetic gypsum after calcination.

The following general relationship was proposed for all the gypsum materials (10):

$$\phi_{ave}(d) = A \cdot ln(d) + B \tag{10}$$

where A and B, are constant equation values.

A very good compatibility of the experimental results with the proposed dependency (10) was obtained in all the cases, which is confirmed by the high values of the R^2 parameter (Table 7).

Table 7. A and B constants of equation (10).

Studied Building Materials	Constants		R^2
	A	B	
Building Gypsum	23.58	22.62	0.9913
Synthetic gypsum before the calcination process	63.29	−166.12	0.9778
Synthetic gypsum after the calcination process	18.28	29.94	0.9784

3.2. The Results of the Setting Time of Gypsum Pastes and Masonry and Plastering Mortars

For the proposed compositions of gypsum pastes (Table 4), measurements of their setting time were made based on the temperature calcination of the synthetic gypsum (Figure 9). In the case of the

measurements of the setting time of the modified gypsum samples, they were made three times for a sample made of the same gypsum pastes. The binding time results were identical, and therefore no statistical considerations were made.

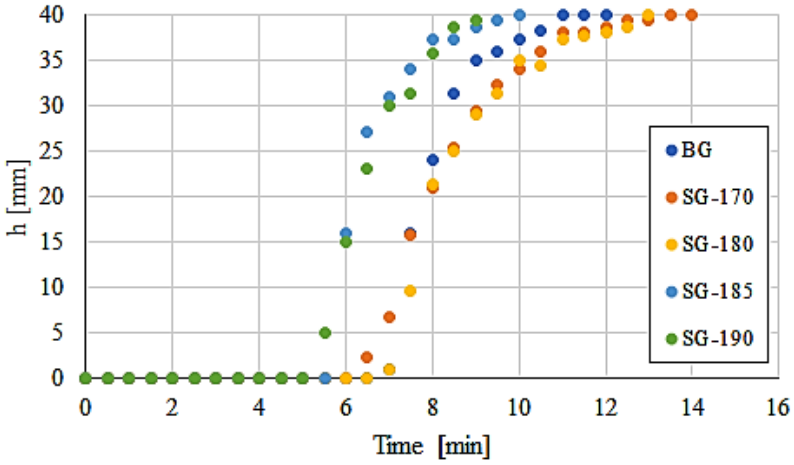

Figure 9. The setting time of the pastes based on the obtained synthetic gypsum. at different calcination temperatures.

The pastes made of gypsum obtained in the calcination process at 170 and 180 °C resulted in longer setting times. The higher gypsum calcination temperature shortened the setting time. During the binding process, the primary hydrates gradually occurred in the form of small crystals (crystallization seeds). The greater the degree of their occurrence, the greater the rate of formation of new crystallization seeds. The pastes with the content of gypsum that was obtained at higher calcination temperatures probably contained increased amounts of crystallization seeds, which accelerated the setting process. Doubts would be unambiguously dispelled by using scanning electron microscope (SEM) photos, but they are not, however, the subject of this publication. Such an analysis should be carried out in the future at the level of the microstructure of the samples.

Based on the measurements of the binding times (initial t_s and final t_e) of the tested synthetic gypsum pastes, the relationships t_s = f(T) and $t_e = f(T)$ were determined.

$$t_p = -\,0.08\,T + 20.4 \tag{11}$$

$$t_k = -\,0.26\,T + 58.5 \tag{12}$$

It was noticed that the setting time was shortened with an increasing calcination temperature of raw gypsum (Figure 10). The beginning of binding for gypsum calcined at 170 °C started in the 7th minute of the setting process and was completed in the 14th minute. However, for gypsum calcined at 190 °C, these times were 5.5 and 9 min, respectively. It is also important that the entire setting process was shortened with the increase of the gypsum calcination temperature. For gypsum calcined at 170 °C, the time between the start and the end of the setting process (Δt = tk−tp) was Δt_{170} = 7 min. In turn, for gypsum calcined at 190 °C, it was only Δt_{190} = 3.5 min.

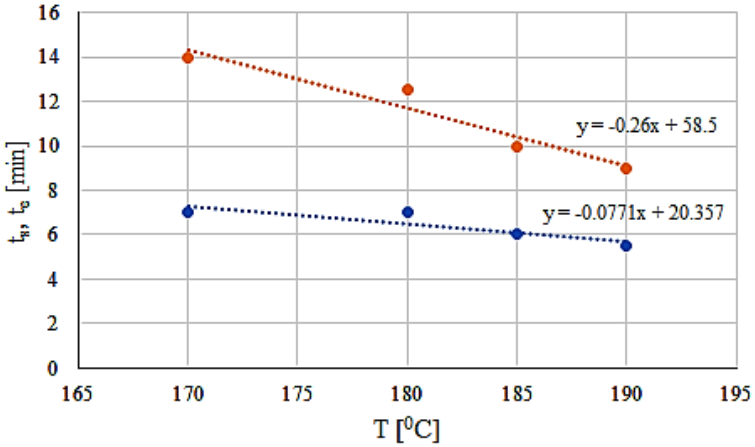

Figure 10. Graph of the dependence between the initial setting time t_s and the final setting time t_e of the synthetic gypsum in a function of its calcination temperature T.

The setting process of the plaster was very fast, and even violent. The beginning of gypsum binding took place just a few minutes after mixing the binder with water, while the end of setting did not exceed 12–14 min. A rapid hydration process adversely affects the microstructure of gypsum material. Therefore, while designing the composition of gypsum mortar mixes (Table 5) and plaster mortar mixes (Table 6), additives that delay the setting process were used. These additives reduced the gypsum solubility and, as a result, extended the setting time. In all the proposed cases of gypsum masonry and plastering mortars, which were based on flue gas desulfurization gypsum, setting times of about 120 min were obtained. This was compliant with the standard requirements for the proposed building materials [48]. The composites show the effect of tartaric acid and Plast Retard on the setting time of building mixes (Table 8).

Table 8. Comparison of the initial values of the setting times t_s of the gypsum pastes and masonry and plastering mortars based on synthetic gypsum with Plast Retard and tartaric acid.

Initial Setting Time (min)				
Gypsum Pastes: BG-Building Gypsum, BS-Synthetic Gypsum				
BG	**SG170**	**SG180**	**SG185**	**SG190**
6.5	7	7	6	5.5
Mortar Based on Building Gypsum with Plast Retard (MBG-PR) Mortar Based on Synthetic Gypsum with Plast Retard (MSG-PR)				
MBG-PR	MSG170-PR	MSG180-PR	MSG185-PR	MSG190-PR
120	120	124	120	120
Mortar Based on Building Gypsum with Tartaric Acid (MBG-A63) Mortar Based on Synthetic Gypsum with Tartaric Acid (MSG-A63)				
MBG-A63	MBG170-A63	MBG180-A63	MBG185-A63	MBG190-A63
120	122	126	120	124
Plastering Mortar Based on Building Gypsum with Plast Retard (PMBG-PR) Plastering Mortar Based on Synthetic Gypsum with Plast Retard (PMSG-PR)				
PMBG-PR	PMSG170-PR	PMSG180-PR	PMSG185-PR	PMSG190-PR
118	120	120	118	118
Plastering Mortar Based on Building Gypsum with Tartaric Acid (PMBG-A63) Plastering Mortar Based on Synthetic Gypsum with Tartaric Acid (PMSG-A63)				
PMBG-A63	PMSG170-A63	PMSG180-A63	PMSG185-A63	PMSG190-A63
126	120	120	118	122

An additional test, not included in the standards, was the determination of the workability time of the mortars. The parameter is the time during which the mortar has not yet started to set, and therefore it shows the ability to easily and accurately fill the forms, while at the same time maintaining homogeneity. During this time, it is possible to put it on a wall and make any corrections resulting from errors arising during construction works. This is a very important feature of fresh gypsum mortars, which translates into the quality of already hardened composites and the products that are made of them.

Figures 11 and 12 additionally summarize the relationship between the setting time and workability of the masonry and plastering mortars that were modified with tartaric acid and Plast Ret in a function of the synthetic gypsum calcination temperature. The figures have the calculated value of 5% error bars marked.

During the comparison of the setting times of the masonry mortars, it was shown that all the mortars containing synthetic gypsum and Plast Retard had a longer workability time when compared to the mortar based on building gypsum. The mortars that contained gypsum, which was obtained in the calcination process at the temperature of 180 °C, had the longest workability time. With the use of A63 type tartaric acid, most of the proposed mortars also achieved a longer workability time. In this case, the longest workability was obtained for the composite based on gypsum calcined at 180 °C (Figure 11).

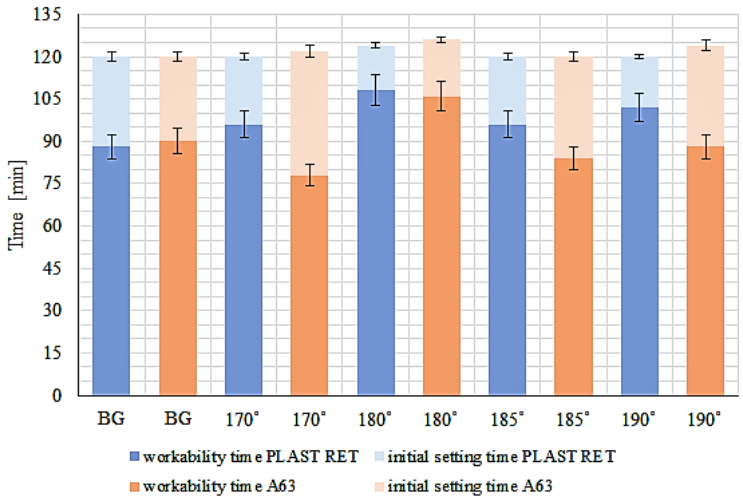

Figure 11. Relationships between the setting times and workability of masonry mortars modified with tartaric acid and Plast Ret as a function of the synthetic gypsum calcination temperature, which was calculated with an error bar value of 5%.

When comparing the setting times of the plastering mortars, it was found that when Plast Retard was used, all the mortars with synthetic gypsum had a longer or comparable workability time to the reference mortar with the building gypsum. When using A63 type tartaric acid, all the mortars were characterized by a constant value of workability time reaching 90 min (Figure 12).

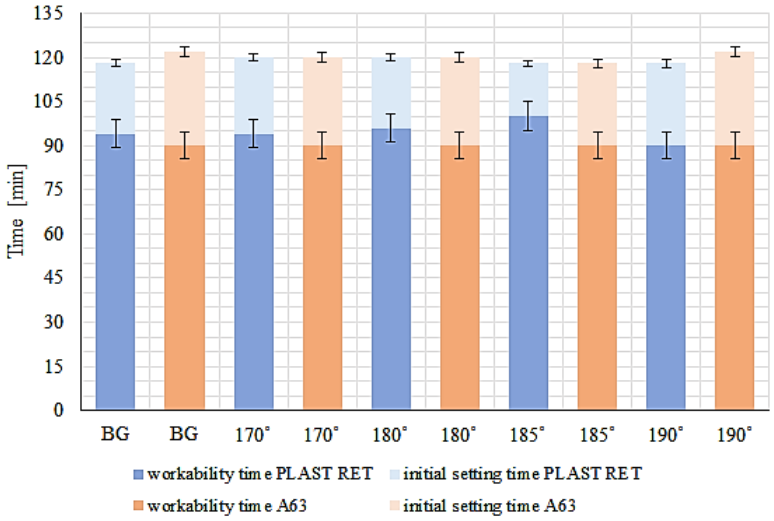

Figure 12. Relationships between the setting times and workability of plastering mortars modified with tartaric acid and Plast Ret as a function of the synthetic gypsum calcination temperature, which was calculated with an error bar value of 5%.

The authors of paper [55] stated that due to the obtained short gypsum setting times, it was necessary to add tartaric acid to mixes with building gypsum. The amount of retarder was empirically selected and determined to be 0.16% of the total dry weight. Sing and Garg [56] also used tartaric acid as a setting retarder for gypsum plasters. They noticed that the used chemicals not only influenced the setting time, but also changed the compressive strength and microstructure of the plaster.

The above parameters are strongly influenced by the pH of the mortar. It was noticed that the pH of the mortar affected the strength of the materials, and the retardation factor was not directly related to the strength of the obtained composites. It was shown that the morphology of the hardened gypsum plaster depends, to a significant extent, on the pH value of the water and the added retarder, and that the maximum compressive strength was achieved when the pH was equal to 7.

In recent years, many research centers have dealt with the influence of the following chemical compounds on setting times: tartaric acid, sodium tartrate, salicylic acid, melamine, sucrose, white cement, sodium triphosphate, citric acid, black tea, and sodium polyphosphate [12,13,57,58]. The results of their work showed that all types of retarders had a different effect on building gypsum, and at the same time they also all had a different effect on gypsum strength.

Paper [14] presents a study of the influence of a composite modifying admixture, which consists of slaked lime and a superplasticizer, on the strength properties and specificity of the shaping of the binder's structure. The compressive strength of the samples made of the modified binders ranged from 20 to 24 MPa, and the flexural strength from 10 to 12 MPa after 28 days. Strength tests of modified gypsum-based building materials are very important from the point of view of construction engineers. The authors of this publication are currently planning research concerning the strength of gypsum materials that are based on synthetic gypsum obtained from flue gas desulphurization.

In turn, the authors of paper [59] analyzed the influence of thermal insulation material on the energy and environmental efficiency of a building. The building was constructed while taking into account the principles of sustainable development, both in terms of its design and technical solutions. In order to assess the impact of the thermal insulation material, various partition configurations were considered, and the original material (glass wool) was replaced with synthetic (polystyrene, polystyrene) and natural materials (wood fiber and kenaf). Moreover, the authors of [60] made improvements to wooden structures with regards to the following: the comfort of use, energy savings, or more broadly speaking, sustainable development. In the context of papers [59,60], it would be advisable to carry out tests of partitions made of materials based on synthetic gypsum (proposed in this paper) with

regards to their thermal and mechanical properties. More advanced construction technologies enable the addition of photocatalysts to gypsum, e.g., TiO_2, in order to obtain a self-cleaning building material and a material with high photocatalytic properties [61].

An important aspect, apart from the mechanical properties, is the search for composites with low thermal conductivity values. Very often, the improvement of thermal properties deteriorates the mechanical properties of materials. A great challenge for scientists is to obtain a material with very good mechanical and thermal properties.

There are current trends in the construction industry of finding new alternatives to traditional functional admixtures for gypsum. Attempts have been made to invent a green and sustainable technology for obtaining innovative composite materials. This approach is conducive to the development of the construction industry towards ecology, energy efficiency and the broadly understood area of energy conservation.

4. Conclusions

The main conclusions of this study are:

- The grain size distribution of the synthetic gypsum before the calcination process differed from that of commercial building gypsum. The synthetic gypsum before the calcination process was characterized by a larger share of particle size within the diameter range of 10–100 μm when compared to the building gypsum, which had particles with diameters from 0.1 to 40 μm. The calcination process caused the grains to break up into smaller diameters. Thanks to this, it was possible to use them when creating masonry and plastering mortars.
- The received statistical parameters of the grain diameters of the synthetic gypsum obtained in the calcination process did not differ from the parameters of the building gypsum. The research allowed the grain diameters of the ecological gypsum in complex multiphase systems, such as pastes and mortars, to be assessed.
- Based on the study of gypsum pastes, for all the samples, a generalized dependence of the mean particle size distribution with regards to the diameter of the tested samples was proposed.
- Pastes made of gypsum that was obtained in the calcination process at 170 and 180 °C resulted in longer setting times when compared to the reference sample that was made of building gypsum. The higher gypsum calcination temperature caused the shortening of the setting time. Correlations that determine the initial and final setting time as a function of calcination temperature were proposed for the tested synthetic gypsums.
- Masonry and plastering mortars based on the synthetic gypsum with the addition of A63 tartaric acid or Plast Retard caused the setting time to be extended to the expected standard values of 2 h, and can be successfully used in innovative building composites. The workability time of all the proposed modified masonry and plastering mortars was nearly equal to 90 min.

Author Contributions: Conceptualization, A.K. and K.P.; data curation, A.K. and K.P.; funding acquisition, A.K.; investigation, A.K. and K.P.; methodology, A.K. and K.P.; writing—original draft, K.P., K.B. and J.C.; writing—review and editing, K.P.; validation, K.B. and J.C.; visualization, J.C.; formal analysis K.B. and J.C.; supervision K.B. All authors have read and agreed to the published version of the manuscript.

Funding: This research was funded by Warsaw University of Technology. Grant supporting research activities for employees of the Warsaw University of Technology in the discipline of Civil Engineering and Transport.

Acknowledgments: This publication was written at the Warsaw University of Technology with the participation of Czech partners from the Technical University in Liberec. This publication was written at the Technical University of Liberec, Faculty of Mechanical Engineering with the support of the Institutional Endowment for the Long Term Conceptual Development of Research Institutes, as provided by the Ministry of Education, Youth and Sports of the Czech Republic in the year 2020.

Conflicts of Interest: The authors declare no conflict of interest. The funders have no role in the design of the study; in the collection, analyses or interpretation of data; in the writing of the manuscript, or in the decision to publish the results.

References

1. Klin, S. Analiza zmienności wytrzymałości i odkształcalności gipsu w różnych stanach naprężeń i wilgotności. *Zesz. Naukowe Akad. Rol. Wroc.* **2005**, *227*, 1–316.
2. Prałat, K.; Kubissa, W.; Jaskulski, R.; Ciemnicka, J. Influence of selected micro additives content on thermal properties of gypsum. *Archit. Civ. Eng. Environ.* **2019**, *3*, 69–79. [CrossRef]
3. Ng, S.; Jelle, B.P.; Zhen, Y.; Wallevik, Ó.H. Effect of storage and curing conditions at elevated temperatures on aerogel-incorporated mortar samples based on UHPC recipe. *Constr. Build. Mater.* **2016**, *106*, 640–649. [CrossRef]
4. Pichniarczyk, P.; Niziurska, M.; Nosal, K.; Wieczorek, M. Wpływ metylocelulozy na mikrostrukturę zapraw gipsowych i cementowych. *Szkło Iceramika.* **2012**, *63*, 12–17.
5. Kocemba, A.; Mucha, M. Zatrzymanie wody i zestalenie w kompozytach gips/polimer. *Przem. Chem.* **2016**, *95*, 1003–1005. [CrossRef]
6. Schiavoni, S.; D'Alessandro, F.; Bianchi, F.; Asdrubali, F. Insulation materials for the building sector: A review and comparative analysis. *Renew. Sust. Energ. Rev.* **2016**, *62*, 988–1011. [CrossRef]
7. Kairies, C.L.; Schroeder, K.T.; Cardone, C.R. Mercury in gypsum produced from flue gas desulfurization. *Fuel* **2006**, *85*, 2530–2536. [CrossRef]
8. Galos, K.A.; Smakowski, T.S.; Szlugaj, J. Flue-gas desulphurisation products from Polish coal-fired power-plants. *Appl. Energy* **2003**, *75*, 257–265. [CrossRef]
9. Głomba, M.; Szmigielska, E. Conversion of calcium carbonate into synthetic gypsum in flue gas desulphurization technology using wet limestone method. *Tech. Trans.* **2011**, *108*, 49–60.
10. Bilici, I. Alternative Evaluation of Synthetic Gypsum with Waste Polyethylene. *Trans. Sci. Technol.* **2018**, *5*, 239–244.
11. DeSutter, T.M.; Cihacek, L.J.; Rahman, S. Application of flue gas desulfurization gypsum and its impact on wheat grain and soil chemistry. *J. Environ. Qual.* **2014**, *43*, 303–311. [CrossRef] [PubMed]
12. Lanzón, M.; García-Ruiz, P.A. Effect of citric acid on setting inhibition and mechanical properties of gypsum building plasters. *Constr. Build. Mater.* **2012**, *28*, 506–511. [CrossRef]
13. Nilles, V.; Plank, J. Study of the retarding mechanism of linear sodium polyphosphates on α-calcium sulphate hemihydrate. *Cement Concr. Res.* **2012**, *42*, 736–744. [CrossRef]
14. Huang, Y.; Xu, C.; Li, H.; Jiang, Z.; Gong, Z.; Yang, X.; Chen, Q. Utilization of the black tea powder as multifunctional admixture for the hemihydrate gypsum. *J. Clean. Prod.* **2019**, *210*, 231–237. [CrossRef]
15. Heim, D.; Mrowiec, A.; Prałat, K.; Mucha, M. Influence of Tylose MH1000 content on gypsum thermal conductivity. *J. Mater. Civ. Eng.* **2018**, *30*, 04018002. [CrossRef]
16. Vimmrova, A.; Keppert, M.; Michalko, O.; Černý, R. Calcined gypsum–lime–metakaolin binders: Design of optimal composition. *Cement Concr. Compos.* **2014**, *52*, 91–96. [CrossRef]
17. Marinkovic, S.; Kostic-Pulek, A. Examination of the system fly ash–lime–calcined gypsum–water. *J. Phys. Chem. Solids* **2007**, *68*, 1121–1125. [CrossRef]
18. Maksoud, M.A.; Ashour, A. Heat of hydration as a method for determining the composition of calcined gypsum. *Thermochim. Acta* **1981**, *46*, 303–308. [CrossRef]
19. Tydlitát, V.; Medveď, I.; Černý, R. Determination of a partial phase composition in calcined gypsum by calorimetric analysis of hydration kinetics. *J. Therm. Anal. Calorim.* **2012**, *109*, 57–62. [CrossRef]
20. Hotta, Y.; Banno, T.; Oda, K. Characteristics of translucent alumina produced by slip casting method using gypsum mold. *J. Mater. Sci.* **2002**, *37*, 855–863. [CrossRef]
21. Shen, Y.; Qian, J.; Zhang, Z. Investigations of anhydrite in CFBC fly ash as cement retarders. *Constr. Build. Mater.* **2013**, *40*, 672–678. [CrossRef]
22. Misnikov, O.; Ivanov, V. Use of Deep Peat-Processing Products for Hydrophobic Modification of Gypsum Binder. In *E3S Web of Conferences*; EDP Sciences: Les Ulis, France, 2017; Volume 15, p. 01017.
23. Kurdowski, W. *Chemia materiałów budowlanych*; AGH Uczelniane Wydawnictwa Naukowo-Dydaktyczne: Kraków, Poland, 2003.
24. Product Card. Available online: https://baza.atlas.com.pl/pliki/pl_5468_20190607_135610.pdf (accessed on 1 November 2020).

25. Crangle, R.D. Gypsum. *Min. Eng.* **2013**, *2013*, 49–50.
26. Ibrahim, T.M.; El-Hussaini, O.M. Production of anhydrite–gypsum and recovery of rare earths as a by-product. *Hydrometallurgy* **2007**, *87*, 11–17. [CrossRef]
27. Evans, T.J.; Majumdar, A.J.; Ryder, J.F.A. Semi-dry method for the production of lightweight glass-fibre-reinforced gypsum. *Int. J. Cement Compos. Lightweight Concr.* **1981**, *3*, 41–44. [CrossRef]
28. Guan, B.; Shen, Z.; Wu, Z.; Yang, L.; Ma, X. Effect of pH on the Preparation of α-Calcium Sulfate Hemihydrate from FGD Gypsum with the Hydrothermal Method. *J. Am. Ceram. Soc.* **2008**, *91*, 3835–3840. [CrossRef]
29. Coppola, L.; Coffetti, D.; Crotti, E. Use of tartaric acid for the production of sustainable Portland-free CSA-based mortars. *Constr. Build. Mater.* **2018**, *171*, 243–249. [CrossRef]
30. Xiaowei, Z.; Chunxia, L.; Junyi, S. Influence of tartaric acid on early hydration and mortar performance of Portland cement-calcium aluminate cement-anhydrite binder. *Constr. Build. Mater.* **2016**, *112*, 877–884. [CrossRef]
31. Yalcin, D.; Ozcalik, O.; Altiok, E.; Bayraktar, O. Characterization and recovery of tartaric acid from wastes of wine and grape juice industries. *J. Therm. Anal. Calor.* **2008**, *94*, 767–771. [CrossRef]
32. Quoc, L.P.T.; Huyen, V.T.N.; Hue, L.T.N.; Hue, N.T.H.; Thuan, N.H.D.; Tam, N.T.T.; Duy, T.H. Extraction of pectin from pomelo (*Citrus maxima*) peels with the assistance of microwave and tartaric acid. *Int. Food Res. J.* **2015**, *22*, 1637.
33. Ruiz-Caro, R.; Veiga, M.D.; Di Meo, C.; Cencetti, C.; Coviello, T.; Matricardi, P.; Alhaique, F. Mechanical and drug delivery properties of a chitosan–tartaric acid hydrogel suitable for biomedical applications. *J. Appl. Polym. Sci.* **2012**, *123*, 842–849. [CrossRef]
34. Zhang, K.; Wang, M.; Wang, D.; Gao, C. The energy-saving production of tartaric acid using ion exchange resin-filling bipolar membrane electrodialysis. *J. Membr. Sci. Res.* **2009**, *341*, 246–251. [CrossRef]
35. Product Card. Available online: http://www.evimex.pl/kwas_winowy_naturalny_z_dodatkiem_antyzb (accessed on 1 November 2020).
36. Wu, C.; Chen, W.; Zhang, H.; Yu, H.; Zhang, W.; Jiang, N.; Liu, L. The hydration mechanism and performance of modified magnesium oxysulfate cement by tartaric acid. *Constr. Build. Mater.* **2017**, *144*, 516–524. [CrossRef]
37. Chen, M.; Guo, X.; Zheng, Y.; Li, L.; Yan, Z.; Zhao, P.; Cheng, X. Effect of tartaric acid on the printable, rheological and mechanical properties of 3D printing sulphoaluminate cement paste. *Materials* **2018**, *11*, 2417. [CrossRef] [PubMed]
38. Pyatina, T.; Sugama, T.; Moon, J.; James, S. Effect of tartaric acid on hydration of a sodium-metasilicate-activated blend of calcium aluminate cement and fly ash F. *Materials* **2016**, *9*, 422. [CrossRef]
39. Product Card. Available online: http://www.evimex.pl/plast_retard_pe (accessed on 1 November 2020).
40. Chen, Q.; Liu, W.; Wang, W.; Thomas, J.C.; Shen, J. Particle sizing by the Fraunhofer diffraction method based on an approximate non-negatively constrained Chin-Shifrin algorithm. *Powder Technol.* **2017**, *317*, 95–103. [CrossRef]
41. Kanwal, R.P. Classical Fredholm Theory. In *Linear Integral Equations*; Springer: New York, NY, USA, 2013.
42. Bentz, D.L.; Hansen, A.S.; Guynn, J.M. Optimization of cement and fly ash particle sizes to produce sustainable concretes. *Cement Concr. Compos.* **2011**, *33*, 824–831. [CrossRef]
43. Coupland, J.N.; McClements, D.J. Droplet size determination in food emulsions: Comparison of ultrasonic and light scattering methods. *J. Food Eng.* **2001**, *50*, 117–120. [CrossRef]
44. Diaz-de-Mera, Y.; Aranda, A.; Notario, A.; Rodriguez, D.; Rodriguez, A.M.; Bravo, I.; Adame, J.A. Submicron particle concentration and particle size distribution at urban and rural areas in the surroundings of building materials industries in central Spain. *Atmos. Pollut. Res.* **2015**, *6*, 521–528. [CrossRef]
45. Hickey, A.J.; Jones, L.D. Particle-size analysis of pharmaceutical aerosols. *Pharm. Tech.* **2000**, *24*, 48–58.
46. ISO, BS. 13320. Particle size analysis—Laser diffraction methods. *ISO Stand. Auth.* **2009**. Available online: https://www.iso.org/standard/44929.html (accessed on 12 October 2020).
47. Prałat, K.; Krymarys, E. A particle size distribution measurements of selected building materials using laser diffraction method. *Tech. Trans.* **2018**, *11*, 95–108. [CrossRef]

48. Polska, P.K.N. *Spoiwa gipsowe i tynki gipsowe—Cz. 2: Metody badań PN-EN 13279-2*; PKN: Plock, Poland, 2006; ISBN 8325110783, 9788325110789.
49. Meng, W.; Valipour, M.; Khayat, K.H. Optimization and performance of cost-effective ultra-high performance concrete. *Mater. Struct.* **2017**, *50*, 29. [CrossRef]
50. Ważyński, P. Badanie wpływu temperatury wyprażania spoiwa gipsowego na wybrane właściwości zapraw budowlanych. Bachelor's Thesis, Politechnika Warszawska, Płock, Poland, 2017.
51. Schaefer, C.O.; Cheriaf, M.; Rocha, J.C. Production of synthetic phosphoanhydrite and its use as a binder in self-leveling underlayments (SLU). *Materials* **2017**, *10*, 958. [CrossRef] [PubMed]
52. Salih, M.A.; Hussein, A.A. Enhancing the compressive strength property of gypsum used in walls plastering by adding lime. *J. Univ. Babylon Eng. Sci.* **2018**, *26*, 58–66.
53. Çakal, G.Ö.; Eroğlu, İ.; Özkar, S. Gypsum crystal size distribution in four continuous flow stirred slurry boric acid reactors in series compared with the batch. *J. Cryst. Growth* **2006**, *290*, 197–202. [CrossRef]
54. Borgwardt, R.H. Calcination kinetics and surface area of dispersed limestone particles. *AICHE J.* **1985**, *31*, 103–111. [CrossRef]
55. Wieczorek, M.; Sobala, M. Ocena możliwości otrzymywania spoiw gipsowo-ettringitowych. *Prace Inst. Szkła, Ceram. Mater. Ogniotrw. Bud.* **2010**, *3*, 177–187.
56. Singh, M.; Garg, M. Retarding action of various chemicals on setting and hardening characteristics of gypsum plaster at different pH. *Cement Concr. Res.* **1997**, *27*, 947–950. [CrossRef]
57. Zhang, Y.; Yang, J.; Cao, X. Effects of several retarders on setting time and strength of building gypsum. *Constr. Build. Mater.* **2020**, *240*, 117927. [CrossRef]
58. Dvorkin, L.; Lushnikova, N.; Sonebi, M.; Khatib, J. Properties of modified phosphogypsum binder. *Acad. J. Civ. Eng.* **2017**, *35*, 96–102. [CrossRef]
59. Bisegna, F.; Mattoni, B.; Gori, P.; Asdrubali, F.; Guattari, C.; Evangelisti, L.; Sambuco, S.; Bianchi, F. Influence of insulating materials on green building rating system results. *Energies* **2016**, *9*, 712. [CrossRef]
60. Švajlenka, J.; Kozlovská, M. Effect of accumulation elements on the energy consumption of wood constructions. *Energy Build.* **2019**, *198*, 160–169. [CrossRef]
61. Janus, M.; Zatorska, J.; Zając, K.; Kusiak-Nejman, E.; Czyżewski, A.; Morawski, A.W. The mechanical and photocatalytic properties of modified gypsum materials. *Mater. Sci. Eng. B* **2018**, *236*, 1–9. [CrossRef]